RSC Advances

ROYAL SOCIETY OF CHEMISTRY

www.rsc.org/advances

Journal Name

RSCPublishing

ARTICLE

Electrospun Hydroxyethyl Cellulose Nanofibers Functionalized with Calcium Phosphate Coating for Bone Tissue Engineering

Cite this: DOI: 10.1039/xoxxoooooox

Received 26th December 2014,
Accepted

DOI: 10.1039/xoxxoooooox

www.rsc.org/

Sugandha Chahal, [a]† Fathima Shahitha Jahir Hussain, [a] Anuj Kumar,[b] Mashitah M. Yusoff [a] and Mohammad Syaiful Bahari Abdull Rasad[c] ,

The aim of this study is to develop a facile and efficient scaffold from electrospun hydroxyethyl cellulose (HEC) functionalized with bone-like calcium phosphate (CaP). The HEC/PVA nanofibers were fabricated by electrospinning and mineralized by incubating in 10× simulated body fluid (SBF) for different period of times. After 24h of incubation, the nanofibers were uniformly coated by a thin layer of mineral deposit. SEM, FTIR, and FESEM-EDS analysis confirm the deposition of CaP on the nanofibers. The nanostructured biomaterial maintained its fibrous and porous structure after mineralization. The XRD results suggest that the deposited mineral phase is a mixture of calcium phosphate hydrate and apatite. The mechanical properties of CaP coated scaffolds has similar tensile strength and elastic modulus with that of trabecular and proximal femoral bones. The cytocompatibility of the CaP coated HEC/PVA scaffolds were evaluated using human osteosarcoma cells. The CaP coated HEC/PVA scaffolds supports cellular attachment and proliferation of osteosarcoma cells and will be a promising candidate for bone tissue engineering.

1. Introduction

Fabrication of scaffold materials by electrospinning has gained great attention for bone tissue engineering. The non-woven mat of electrospun nanofibers can serve as an ideal scaffold to mimic the extracellular matrix (ECM) for cell attachment and nutrient transportation owing to its high porosity and large surface-area-to-volume ratio.[1] Various polymers have been investigated for bone tissue engineering including collagen, chitin, PDLLA, PLGA, and PCL.[2-4] Naturally human bone is a mixture of organic-inorganic composite. The organic part consists of collagen fibrils, embedded in arrayed structure by the nanocystalline rod-like inorganic component which is hydroxyl-apatite (HA).[5-6]

Treatment of simulated body fluids (SBF) is frequently used for the formation of apatite on the surface of biomaterials. SBF is an electrolyte solution having inorganic composition similar to human blood plasma. SBF have the ability to form calcium phosphate containing apatite on the surface of artificial biomaterials.[7] Different composition of SBFs have been prepared to deposit CaP minerals on engineered biomaterial including fibrous scaffolds,[8,9] and solid implants.[10,11] The conventional SBF mimics the human blood plasma in the ion concentrations of Ca^{2+}, HPO_4^{2-}, Na^+, Cl^-, K^+, Mg^{2+}, and SO_4^{2-} except with a significant deficiency in its HCO_3^- concentration (4.2 mM, while it is 27 mM in the human blood plasma).[12]

Cellulose with its β-1,4 glycosidic bond, is an excellent material for tissue engineering applications.[13] Last few years the use of cellulose based material specially cellulose nanocrystals has been widely investigated for tissue engineering applications due to their excellent biocompatibility, biodegradability and low cytotoxicity.[14-16] Hydroxyethyl cellulose (HEC), one of the leading cellulose derivative is extensively used in various fields such as pharmaceutical industries,[17] paints,[18] and emulsion polymerizations.[19] It is non-ionic, water soluble polymer with β-glucose linkage, which makes it a suitable candidate for tissue engineering applications. Due to the non-ionic nature, electrospinning of HEC polymer solution is very difficult, so HEC should be electrospun with an electrospinable polymer.

Poly(vinyl alcohol) (PVA) has gained acceptance as a scaffold supporting material for tissue engineering applications.[20] It provides mechanical stability and flexibility to the conventional scaffolds made of natural polymers.[21] In addition, PVA hydrogels have been used in a number of biomedical applications including cartilage implants,[22] soft contact lenses,[23] artificial organs,[23] and drug-delivery matrices. Our research group has been working on the HEC/PVA based nanofibrous scaffolds applications in skin tissue engineering[24] and bone tissue engineering.[24]

In our previous work,[25] we have synthesized the CaP coated HEC/PVA nanofibrous scaffolds and the present work is predominantly focused on the evaluation of mechanical

properties and cytocompatibility of CaP coated nanofibrous scaffolds.

2. Experimental

2.1. Materials

Hydroxyethyl cellulose (HEC) (M.W 90,000) was purchased from Sigma-Aldrich. The partially hydrolyzed poly (vinyl alcohol) (PVA) (average molecular weight 20,0000) was purchased from Merck, Germany. The chemicals needed for SBF solution such as NaCl, KCl, $CaCl_2.2H_2O$, $MgCl_2.6H_2O$, $NaH_2PO_4.H_2O$, and $NaHCO_3$ were procured from Merck, Germany.

2.2. Electrospinning

HEC solution (4wt %) was prepared by dissolving HEC powder in de-ionized water with continuous stirring for 6 h. PVA solution (11 wt %) was prepared in de-ionized water with continuous stirring at 80 °C for 2 -3 h. Blend solution of HEC and PVA were prepared by mixing HEC and PVA at 50:50 ratio with continuously stirring for 12-24 h. The polymer solutions were electrospun at 20 kV, at a rotation speed of 2000 rpm with a tip-to-collector distance of 13 cm using a flow rate of 1 ml/h. The nanofibers were cross-linked with glutaraldehyde to make them water insoluble before mineralisation process and cell seeding.

2.3. CaP mineral deposition on nanofibers

10x simulated body fluid solution were prepared according to Tas and Bhaduri[7] and Mavis et al.[26] The chemical composition of 10x SBF solutions is listed in Table 1. The stock solution was prepared by adding the first five chemicals until complete dissolution of each reagent in 900ml de-ionized water by continuous stirring at room temperature. For mineralization, 200 ml of the stock solution was transferred into a beaker and 0.168 g of $NaHCO_3$ was added and $1cm^2$ HEC/PVA nanofibrous scaffolds were immersed in the solution for 12, and 24 h at room temperature after that they were rinsed with de-ionized water to remove the salt residues.[27]

Table 1: Reagents for preparing 1 L of 10x SBF solution.

Order	Reagent	Amount (g)	Molarity (mM)
1	NaCl	58.443	1000
2	KCl	0.373	5
3	$CaCl_2.2H_2O$	3.675	25
4	$MgCl_2.6H_2O$	1.016	5
5	$NaH_2PO_4.H_2O$	0.250	3.62
6	$NaHCO_3$	0.840	10

2.4. Characterizations

The surface morphology of the scaffolds were observed using scanning electron microscopy (SEM, ZEISS-EVO 50) at an accelerating voltage of 10 kV was used. The pore sizes were estimated according to methods reported in She et. al. [28] using image processing software *ImageJ* (National Institute of Health, Maryland, USA).

FTIR analysis was performed using Thermo Nicolet 6700 in the absorbance range of 600-4000cm^{-1} with 32 scans per run to estimate the bond formation. XRD spectra were obtained by Rigaku D/max X-ray diffractometer with Cu Kα-radiation (2500VB2+/PC, 40 kV, 200 mA). The scanning range was from 3 to 60^o with a step size of 0.2^o. TGA was performed using Toledo STAR-1 (Mettler; Switzerland). About 5 mg of sample was heat treated from 30 to 900 ^{o}C at a heating rate of 10 ^{o}C/min under nitrogen atmosphere.

Tensile strength of electrospun nanofibrous scaffolds was measured with a universal testing machine (LabTest 4.100SP1, Czech Republic) using load cell of 100 N capacity. Rectangular specimen of dimensions 10 mm × 30 mm was used for testing, at a crosshead speed of 5 mm/min and the data were recorded for every 50μs. The elastic moduli were calculated based on the obtained tensile stress–strain curve. The values were obtained from the average of 15 samples for (n=10) each type of scaffolds.

2.4.1. Cell culture and adhesion study for cytocompatibility of scaffolds

Human osteosarcoma cells (ATCC, VA, USA) were grown in MEM (Gibco, USA) supplemented with 10% fetal bovine serum and 1% penicillin/ streptomycin. The cells were maintained in a humidified incubator at 37^{0}C with 5% CO_2. Before cell seeding, the scaffolds were sterilized under ultraviolet (UV) light for 60 min, followed by immersion in 70% ethanol for 30 min. The scaffolds were washed with phosphate buffered saline (PBS, Sigma Chemical Co., USA) thrice to eliminate any residual ethanol and soaked in cell culture medium for 2 h. Confluent stock cultures of cells were harvested with 0.05% (v/v) trypsin-EDTA and then seeded on to the scaffolds at a density of 1×10^4 cells / well and incubated in an atmosphere of 5% CO_2 at 37 ^{o}C. The medium was replenished every second day to ensure that there was an adequate supply of nutrients present in the culture plate.

To assess the morphology of cells, the cell/scaffolds construct were washed with 0.1M PBS twice and fixed with 2.5% glutaraldehyde for 10 minutes at room temperature and dehydrated through increasing concentration of ethanol.

Cell proliferation was quantified by Cell Titer 96® Aqueous One Solution Cell Proliferation Assay (MTS Assay) (Promega, Madison, WI, USA). After 1, 3 and 7 days, the media were washed with 0.1 M PBS then 300μl of fresh media and 60 μl of the MTS solution were added to each well and incubated at 37^{o}C for 3 hours. Finally, 200 μl of the mixture was collected and transferred in to a 96-well plate to record the absorbance at 490 nm using a Vmax Microplate reader. The reported data are averaged over two sets of assays and six replicates of each material per set were used.

2.5. Statistical Analysis

The one way ANOVA was performed by using Origin (Lab 9.1, USA) statistical data analysis software to calculate the samples mean difference and standard deviations at $P < 0.001$ level for the mechanical properties and cell viability analysis.

3. Results and discussions

3.1. Morphological Characterizations

The morphology of HEC/PVA nanofibers is smooth and relatively uniform. The HEC/PVA nanofibers exhibited a nonwoven fibrous structure, randomly oriented as shown in Figure 1(a). The nanofibers having the well-developed porous structure is shown in Figure 1(a) (inset).The average diameter of nanofibers (n=110) is 300 ± 20 nm, which is estimated using *ImageJ* image processing software.

After 12 h of incubation in SBF the mineral deposition was found over the surface of nanofibers like crystals of nanoflowers, deposited in small patches as seen in Figure 1(b) (and the inset shows more magnified image of CaP flakes attached with nanofibers). Further, the Figure 1(c) shows the increased mineral deposition after 24 h of treatment in SBF. For 24 h of incubation the crystal size increased, and covered the nanofibers fully with more uniform shapes. The weight of the nanofibers also increased with the incubation time by 36% and 76% for 12 h and 24 h dipping in SBF respectively.

The pore size of the scaffolds plays a critical role in bone formation in vitro and in vivo. In this study, the pore size was estimated using image processing technique as described by She et. al .[28] The pore size of HEC PVA 50 50 electrospun scaffold is 8.834 ± 1 µm estimated using Figure 2a, the mean value of 100 points measurement. Similarly, the mean pore size of CaP coated nanofibers are 5.7 µm and 4.9 µm after 12 h and 24 h incubation time period respectively. The pore size of the electrospun scaffolds decreases with incubation time, as clearly seen in Figure 2 (b,c), the black colour (pore size) decreases due to the CaP coating.

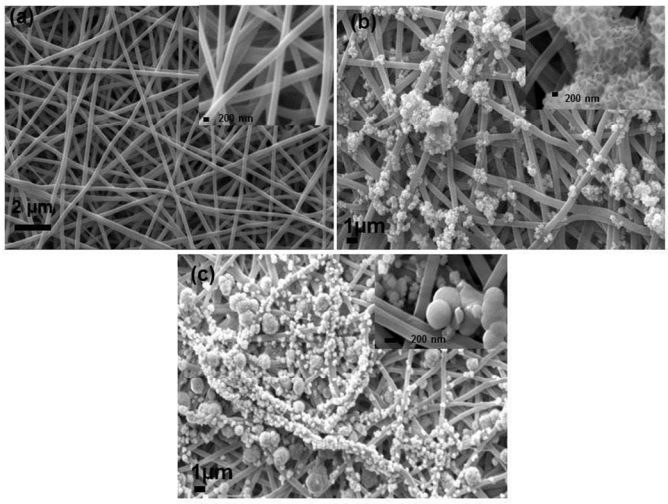

Figure 1. SEM micrographs of electrospun scaffolds (a) HEC/PVA, (b) 12 h SBF treated and (c) 24 h SBF treated.

3.2. Chemical characterization of scaffolds

For HEC/ PVA 50:50 nanofibers the characteristic stretches of HEC are shown (Figure 3) in the 828.71-849.60 cm^{-1} region. The C-O-C stretching vibrations appear at 1422-1426.12 cm^{-1}. The secondary hydroxyl group for HEC appears at 1724.65-1729.45 cm^{-1} and the –C-OH in plane stretching at 1373.24-1374.86 cm^{-1}. The main functional groups of HEC are present even after electrospinning it with PVA.

The peak between 3550-3200 cm^{-1} shows the O-H from intermolecular and intramolecular hydrogen bonds in PVA molecules. The C-H alkyl groups are present near 2850-3000 cm^{-1}, the C-O-C sequence of amorphous PVA appears at 1093.65 cm^{-1}.[29,30] The C-O crystallinity peaks of PVA at 1141 cm^{-1} are not appearing in electrospun nanofibers HEC.

The FTIR spectra of nanofibers treated with 10 x SBF at different time periods are shown in Figure 3. The characteristic absorption bands of PO_4 are formed as P-O stretching at 1024.89 cm^{-1} for 12 h treatment; 1022.00 and 1131.69 cm^{-1} for 24 h[7] and these bands correspond to the commercial HA.[26] The additional characteristic peaks of PO_4 appears at the 950-960 cm^{-1} and at 602.5 and 607.3 cm^{-1} for SBF treated scaffolds. The peaks between 3500-3400 cm^{-1} and 1650 cm^{-1} are attributed to O-H stretching and bending respectively for water molecules existing in the unit cell of di-calcium phosphate dehydrate,[27] concluded that with increase in dipping time the PO_4 percentages increases, as clearly seen with increase in the peak intensity. After the depositions of calcium phosphate particles, the broad peaks at 1085.35 cm^{-1} of C-O-C sequence of PVA shifted to 1135.5 cm^{-1}. On the other hand all other peaks of HEC and PVA remained the same even after calcium phosphate coating.

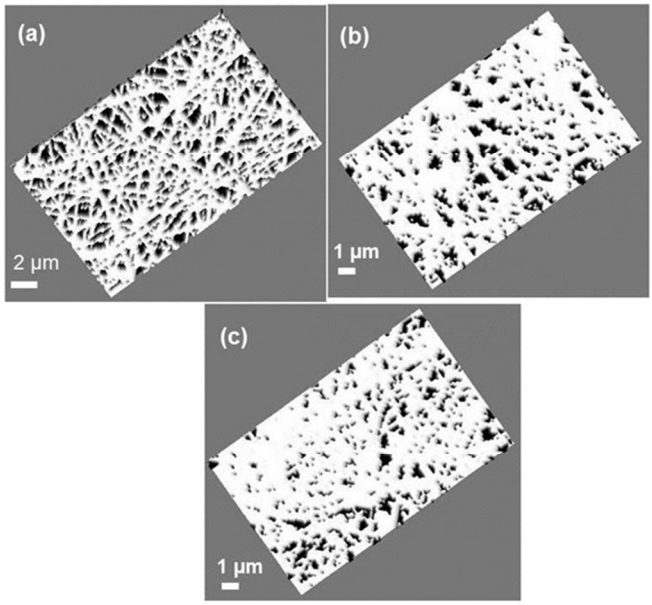

Figure 2. 3D threshold SEM micrographs of electrospun scaffolds that were used to calculate the pore size (dark color) (a) HEC PVA, (b) 12 h SBF treated and (c) 24 h SBF treated.

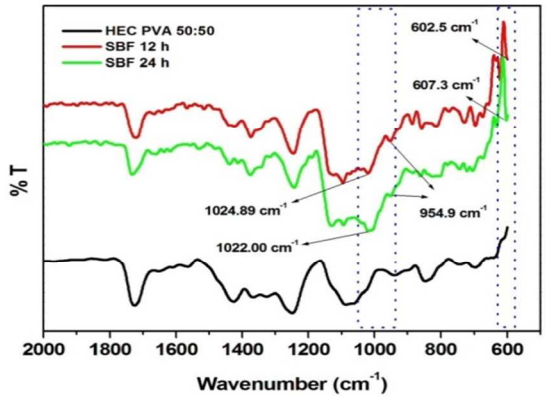

Figure 3. FTIR spectra of HEC/PVA and CaP coated scaffolds at different time periods.

3.3. XRD analysis

Figure 4 shows the diffraction peak at 22° which corresponds to intermolecular interference between PVA chains in the direction of the intermolecular hydrogen bonding in the electrospun scaffolds. After 12 h and 24 h SBF dipping, the scaffold show different X-ray diffraction peaks. The 12 h SBF treated scaffolds shows three X-ray peaks at 14.2°, 16.9° and 25.65° representing β−tri-calcium phosphate, hydroxyapatite (101) [11008 (ICDD)] and hydroxyapatite (002) respectively. As dipping time increases, more amount of hydroxyapatite is deposited uniformly on scaffolds. The increased deposition of mineral is clearly shown in X-ray diffraction result in Figure 4. The 24 h SBF soaked scaffolds show extra five diffraction peaks compared to 12 h soaked scaffolds at 4.50° (hydroxyapatite), 21.133° (Calcium Phosphate Hydrate), 23.489° (hydroxyapatite), 29.325° (hydroxyapatite, 120) and 32.13° (hydroxyapatite, 211). Similar type of results was reported in the literature.[31-33]

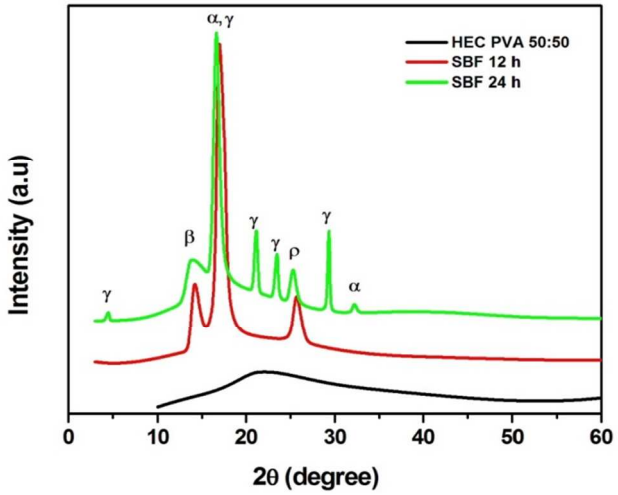

Figure 4. X-ray pattern of HEC/PVA, and CaP coated scaffolds. The symbols, α = Calcium Phosphate Hydrate; β= β−tri-calcium phosphate and γ = hydroxyapatite.

3.4. Energy Disperse X-ray analysis (FESEM-EDX)

The EDX results revealed the percentages of phosphors and calcium on the HEC/PVA scaffolds after SBF treatment for different time periods. Figure 5(a) shows the EDX of scaffolds that were treated in SBF for 12h and the average (n=4) percentage of calcium and phosphors were 14.5% and 8.65% respectively. The percentage of carbon and oxygen were high compare to Ca and P, because at 12 h SBF dipping period the Ca and P did not cover the whole area of the scaffolds. On the other hand, the higher percentage of Ca and P accumulate on the scaffolds surface after 24 h SBF dipping. The average percentage of Ca and P were 17.9% and 35.74% respectively as shown in Figure 5(b).

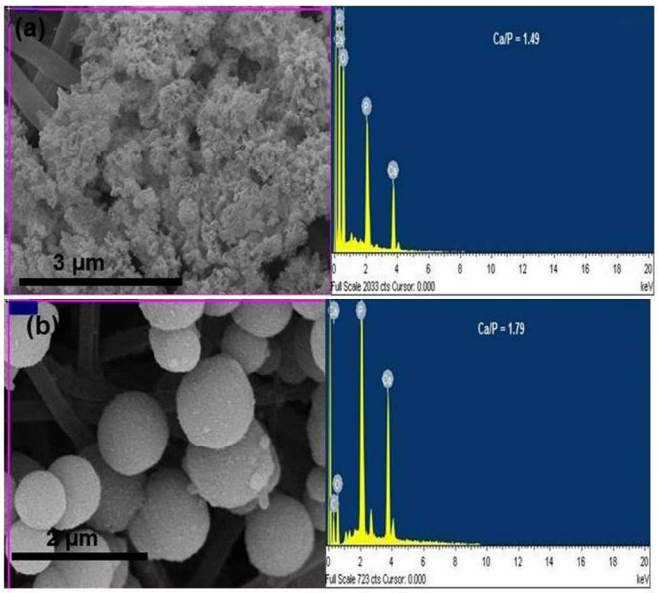

Figure 5. FESEM-EDX of HEC/PVA/CaP scaffolds treated in SBF for (a) 12 h and (b) 24 h.

3.5. Thermogravimetric analysis

Figure 6 (a) shows the typical TGA thermograms for electrospun scaffolds as the function of temperature, with and without mineral coating. The samples were tested in the temperature range from 30 °C up to 900 °C with a constant rate of 10 °C/min under nitrogen atmosphere. The TGA results shows that all samples exhibited three distinct weight loss stages at 30 - 210 °C (5 wt% loss of weakly adsorbed water), 210 – 400 °C (decomposition of side chain of PVA) and 400–540 °C (decomposition of main chain of PVA). Major weight losses are observed about 75 wt% in the range of 210-540 °C for all samples, which are corresponds to the structural decomposition of PVA and it is due to the dehydration and de-polymerisation of PVA chain in the absence of oxygen.[34] According to the literature the maximum peak temperature of pure PVA is around ~323 °C [35] but this peak of PVA is shifted to lower temperature ~289 °C due to the presence of HEC, as shown in Figure 6(b). For fibers treated in SBF for 12h and 24h the maximum peak temperature again shifted to higher temperature as 305 and 342 °C respectively.

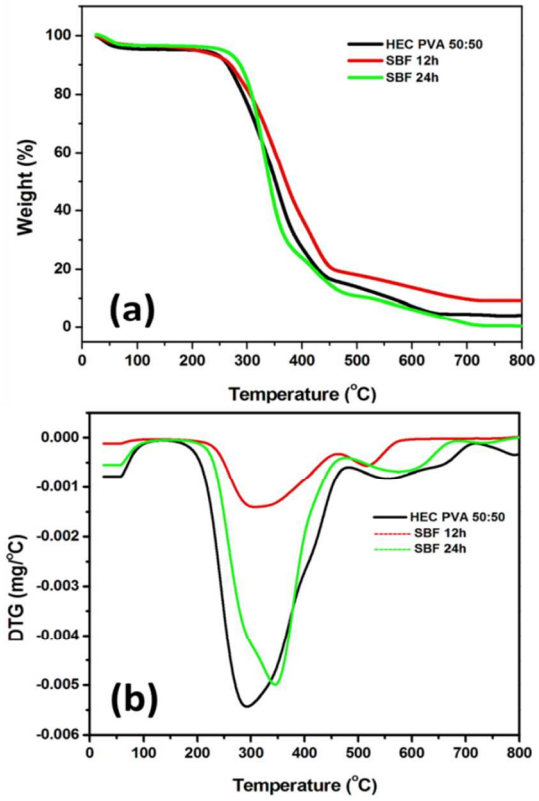

Figure 6. TGA (a) and DTG (b) peaks of HEC/PVA scaffolds and calcium phosphate coated HEC/PVA scaffolds.

3.6. Mechanical characterization

The tensile properties i.e. tensile strength and elastic modulus of electrospun HEC/PVA and CaP coated HEC/PVA scaffolds are shown in Figure 7(a). The blend HEC/PVA scaffolds (crossed-linked) shows an average tensile strength of 3.3 ± 0.10 MPa, the CaP coated HEC/PVA scaffolds after 12h and 24 h dipping shows 3.8 ± 0.10 MPa and 4.2 ± 0.10 MPa respectively. The tensile strength of HEC/PVA electrospun scaffolds increase with SBF incubation time, 15 % for 12h and 27% for 24 h. The biomimetic coating of calcium phosphate minerals like hydroxyapatite,[36,37] and nano hydroxyapatite,[38,39] has enhanced the mechanical strength of electrospun scaffolds.[36-39] The average elastic modulus of HEC/PVA scaffolds is 355 ± 10 MPa, and for HEC/PVA treated with SBF for 12h and 24h are 368 ± 12 MPa and 412 ± 12 MPa respectively. After 24h of dipping in SBF both the tensile strength and elastic modulus of scaffolds significantly improved at $P < 0.001$ level to HEC/PVA scaffolds. The increase in elastic modulus could be attributed to an increase in rigidity over the HEC/PVA scaffolds when the CaP is coated, resulting in strong adhesion at the materials.[39]

Similarly, the tensile stress of HEV/PVA electrospun scaffolds are lower compared to CaP coated scaffolds as clearly shown in stress-strain curve (Figure 7 b). But the elongation at break in stress-strain curve is drastically decreased from 27 to 12 % and 10% for 12 h and 24h treated scaffolds respectively. This decrease in elongation at break is because the CaP coating increase the brittleness of electrospun scaffolds as reported by Thomas *et.al* [39]. Yang *et* al.[45] also reported the significant enhancement of PCL nanofibers tensile strength and elastic modulus after the mineralization in SBF solution.

However, the mechano-morphological properties suggest that HEC/PVA and HEC/PVA/CaP electrospun scaffolds are potential candidate materials for bone regeneration of low and/or non-load bearing areas, because the load-bearing natural bone has very high tensile properties as mentioned in the literature.[40,41] The tensile strength and elastic modulus of trabecular bone (proximal tibia) are 5.3 MPa and 445 MPa respectively.[42] Similarly, the proximal femoral bone has tensile strength of 6.8 MPa and elastic modulus of 441 MPa.[43] The CaP coated HEC/PVA scaffolds has almost similar properties like trabecular and proximal femoral bones.

During the deformation process the CaP nanoparticles orient and align under tensile stress, creating temporary cross-links between polymer chains, thereby creating a local region of enhanced strength. This mechanical reinforcement effect can be attributed to an additional energy-dissipating mechanism introduced by the CaP nanoparticles in HEC/PVA nanofibers Shah *et* al.[44] molecular dynamics studies also suggest that this additional dissipative mechanism is a result of the mobility of the nanoparticles. Yang et al.[45] also reported the significant enhancement of PCL nanofibers tensile strength and elastic modulus after the mineralization in SBF solution.

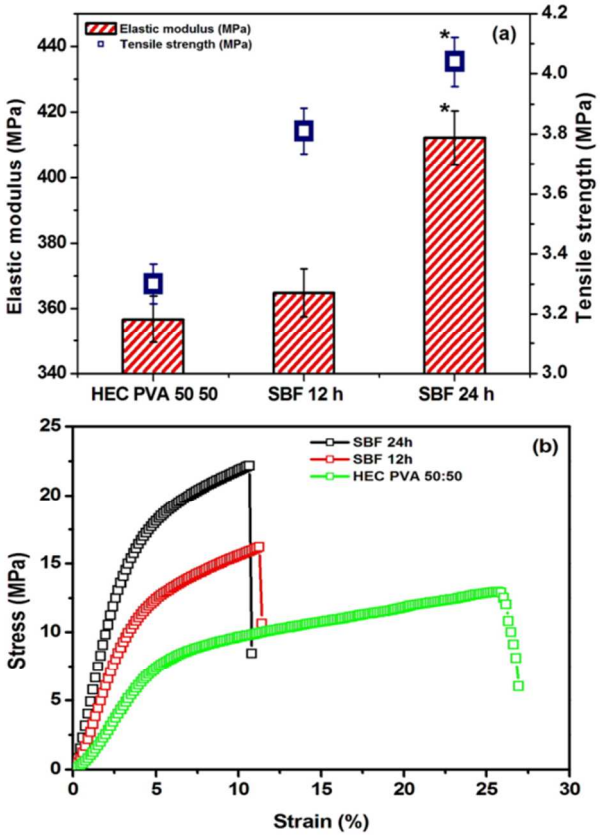

Figure 7. Tensile properties of HEC/PVA and CaP coated HEC/PVA scaffolds, (a) tensile strength, & elastic modulus and, (b) stress-strain curve of scaffolds. *Significant difference at $P < 0.001$.

3.7. Cells morphology and cells proliferation

The SEM images reveal that the cells appear flat and exhibit intact, well-defined morphology with cell coverage increasing with time (Figure 8). SEM images of osteosarcoma cells cultured for 1 and 3 days on both of the CaP coated and HEC/PVA scaffolds as shown in Figure 8. The cells with flattened morphology and many protruding extensions making cell-surface focal contacts with HEC/PVA scaffolds are seen after 1 day of cell seeding (Figure 8a) and after 3 days (Figure 8d) they are covering the surface of the scaffold and proliferating through the pores. The 12 h CaP coated sample show the flattened shape morphology after 1 day (Figure 8b) and after 3 days of seeding (Figure 8e) cells spread more on CaP coated surfaces. The interaction of cell with coated fibers is shown in Figure 8g at higher magnification.
The scaffolds treated in SBF for 24h have higher CaP deposition compared to 12 h, but there is not much difference in the cells proliferations. Figure 8(c, f) shows the cells attachment on 24 h SBF incubated sample for 1 and 3 days after cells seeding. In Figure 8f, the cells are growing on the CaP coated surface and start forming a 3D shape only after 3 days seeding. The osteosarcoma cells spread and migrate on the surface of scaffolds with CaP coating.

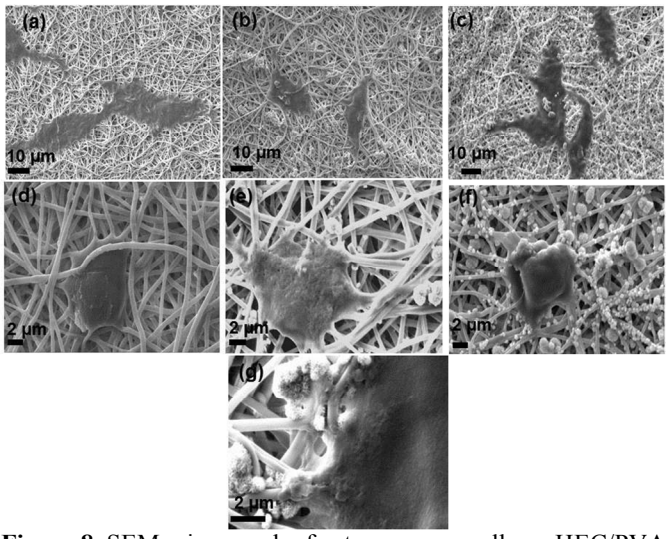

Figure 8. SEM micrograph of osteosarcoma cells on HEC/PVA and CaP coated scaffolds for different days. HEC/PVA (a) 1 day and (d) 3 day; 12 h SBF treated (b) 1 day, (e, g) 3 days and 24 h SBF treated (c) 1 day and (f) 3 days.

Further, the MTS assay was used to quantify cell proliferation on the electrospun scaffolds. Figure 9 shows the cell proliferation of osteosarcoma cells on HEC/PVA and CaP coated scaffolds for 1, 3 and 7 days of cells seeding. The optical density of cells increase with the number of days for each type of electrospun scaffolds, at 1 day of cells seeding there are no significant difference ($P < 0.001$) in mean values of optical densities for the scaffolds. The optical density of cells for 12 h CaP coated scaffolds is significantly higher ($P < 0.001$) than HEC/PVA scaffolds for 7 days cells seeding. It is clear that the optical density for 24h CaP coated scaffolds are significantly higher ($P < 0.001$) than that obtained from the HEC/PVA scaffolds after 3 and 7 days, as shown in Figure 9. Hence, it is clearly observed that the cell adhesion and proliferation increased with time period on both CaP coated and uncoated HEC/PVA scaffolds.

Calcium phosphate-coated nanofibrous polymeric scaffolds has enlarged the scope of bone tissue engineering research, mimicking nanoscale architecture and chemical composition of native bone ECM.[46, 47] SBF incubation is widely used and is an effective way to introduce bone-like apatite onto nanofibrous scaffolds. However, the process is time-consuming and usually requires a few weeks to complete. But for the significant enhancement of coating formation with lesser time, in this work we have used 10 X SBF which has 10 times calcium and phosphate concentration as compared to conventional SBF.[7] The TGA results (Figure 6) confirmed the sufficient mineralization on scaffolds up to 20% by weight of scaffolds for 24 h incubation time.

The mineralization of nanofibrous scaffolds was sensitive to the surface chemistry or functional groups present in scaffolds, diameter of fibers and time of incubation. The HEC/PVA nano fibrous have small diameter (300 ± 20 nm), and the presence of abundant carboxyl groups (due to the crosslinking) on nanofibers provide nucleation sites for Ca^{2+} for CaP deposition. In earlier studies, it was demonstrated that nanofibers diameter[48,49] play an important role for CaP deposition i.e. smaller the nanofibers diameter more the CaP quantity deposited.The EDS (Figure 5) revealed the CaP increase with the incubation time and the XRD (Figure 4) analysis confirmed the formation of extra peak for calcium phosphate hydrate and hydroxyapatite.

The natural bone material is a mineralized connective tissue that shares some common structural characteristics and fulfils diverse mechanical functions. A characteristic elementary unit of bone is the mineralized collagen fibril. The mineralized fibril, together with non-collagenous proteins and water, arranged in a complex hierarchical structure, are ultimately responsible for the mechanical properties of the material.[50-52] The prepared HEC/PVA nanofibrous scaffolds possess excellent nanoscale architecture with interlinked porous structure and the porous structure was maintained even after CaP coating (Figure 1a). The HEC/PVA nanofibrous architecture provides a highly elastic template for mineralization and cell proliferation like collagen type I in natural ECM. Further CaP coating enhanced the mechanical stiffness (Figure 7) and osteoconductivity of scaffolds (Figure 8 and 9).

4. Conclusions

In conclusion, the CaP deposition has enhanced the tensile properties of HEC/PVA nanofibers significantly. Analysis of cell-scaffolds interactions indicated that osteosarcoma cells adhere well on HEC/PVA scaffolds although having lower proliferation compared to CaP coated scaffolds because of lesser surface roughness and lack of bone like minerals. The CaP coated scaffolds have significant improved cell proliferation. The CaP coated HEC/PVA scaffolds are promising material for bone tissue regeneration due to its structure which is similar to natural bone ECM.

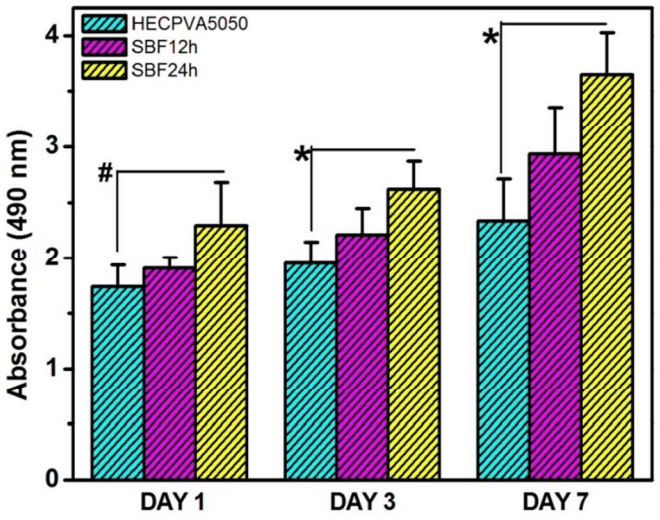

Figure 9. The osteosarcoma cells proliferation on HEC/PVA and CaP coated scaffolds after 1, 3, and 7 days cells seeding. * Significant difference at $P < 0.001$ and # not significant difference at $P < 0.001$.

Acknowledgements

Authors wish to thanks Mr Tomàš Vlach and Ms Lenka Laiblová for helping in conducting the tensile properties estimation at Czech Technical University in Prague, Czech Republic. This work was supported by Fundamental Research Grant Scheme (FRGS) RDU100106, by Ministry of Higher Education, Malaysia.

Notes and references

[a] Faculty of Industrial Sciences and Technology, Universiti Malaysia Pahang, LebuhrayaTun Razak, 26070 Gambang, Kuantan, Pahang.

[b] Czech Technical University in Prague, Faculty of Civil Engineering, Department of Building Structures, Thákurova 7, 16629, Praha 6, Czech Republic.

[c] Department of Biomedical Science, Kulliyyah of Allied Health Sciences, IIUM, 25200 Kuantan, Pahang, Malaysia.

† Corresponding author: Email- mlt.mony@gmail.com

(1) Zhang, Y.; Ouyang, H.; Lim, C. T.; Ramakrishna, S.; Huang, Z. M. Electrospinning of gelatin fibers and gelatin/PCL composite fibrous scaffolds. *J Biomed Mater Res Part B: Appl Biomater* **2005**, *72B*, 156–165

(2) Zhang, Y. Z.; Wang, X.; Feng, Y.; Li, J.; Lim, C. T.; Ramakrishna, S. Coaxial electrospinning of (fluorescein isothiocyanate-conjugated bovine serum albumin)-encapsulated poly (ε-caprolactone) nanofibers for sustained release. *Biomacromolecules* **2006,** *7,* 1049–1057.

(3) Zhang, Y. Z.; Venugopal, J.; Huang, Z. M.; Lim, C. T, Ramakrishna, S. Characterization of the surface biocompatibility of the electrospun PCL-collagen nanofibers using fibroblasts *Biomacromoecules* **2005***,* *6*, 2583–2589.

(4) Poinern, G. E.; Brundavanam, R. K.; Mondinos, N.; Jiang, Z. T. Synthesis and characterisation of nanohydroxyapatite using an ultrasound assisted method. *Ultrason Sonochem* **2009,** *16,* 469–74.

(5) Weiner, S.; Wagner, H. D. The material bone: Structure-Mechanical Function Relations. *Annu Rev Mater Sci.* **1998,** *28*, 271–98.

(6) Hellmich, C.; Ulm, F. J. Average hydroxyapatite concentration is uniform in the extracollagenous ultrastructure of mineralized tissues: evidence at the 1-10-microm scale. *Biomech Model Mechanobiol.* **2003,** *2,* 21–36.

(7) Tas, A. C.; Bhaduri, S. B. Rapid coating of Ti6Al4V at room temperature with a calcium phosphate solution similar to 10× simulated body fluid. *J Mater Res* **2004,** *19(9),* 2742-2749.17

(8) Yang, F.; Wolke, J. G. C.; Jansen, J. A. Biomimetic calcium phosphate coating on electrospun poly(ε-caprolactone) scaffolds for bone tissue engineering. *Chem Eng J* **2008,** *137,* 154–161.

(9) Madurantakam, P. A.; Rodriguez, I. A.; Cost, C. P, Viswanathan, R.; Simpson, D. G.; Beckman, M. J, et al. Multiple factor interactions in biomimetic mineralization of electrospun scaffolds. *Biomaterials* **2009***, 30*, 5456–5464.

(10) Zhang, R.; Ma, P. X. Porous poly (L-lactic acid)/apatite composites created by biomimetic process *J Biomed Mater Res* **1999,** *45*, 285–293.

(11) Murphy, W. L.; Kohn, D. H, Mooney, D. J. Growth of continuous bonelike mineral within porous poly(lactide-co-glycolide) scaffolds in vitro. *J Biomed Mater Res* **2000,** *50*, 50–58.

(12) Kokubo, T.; Takadama, H. How useful is SBF in predicting in vivo bone bioactivity? *Biomaterials* **2006,** *27,* 2907–2915.

(13) Azizi Samir, M. A. S.; Alloin, F.; Dufresne, A. Review of recent research into cellulosic whiskers, their properties and their application in nanocomposite field. *Biomacromolecules* **2005,** *6,* 612−626.

(14) Kmmerer, K.; Menz, J.; Schubert, T.; Thielemans, W. Biodegradability of organic nanoparticles in the aqueous environment. *Chemosphere* **2011,** *82*, 1387−1392.

(15) Kovacs,T.; Naish, V.; O'Connor, B.; Blaiseagn, C.; Hall, L.; Trudeau, V.; Martel, P. An ecotoxicological characterization of nanocrystalline cellulose (NCC). *Nanotoxicology* **2010,** *4*, 255−270

(16) Domingues, R. M. A.; Gomes, M. E.; Reis, R. L. The potential of cellulose nanocrystals in tissue engineering strategies. *Biomacromolecules* **2014,** *15*, 2327−234618

(17).Radebaugh, W. G.; Murtha, L.; Julian, T. N.; Bondi, J. N. Methods for evaluating the puncture and shear properties of pharmaceutical polymeric films. *Int J Pharm* **1988,** *45*, 39-46.

(18).Kroon, G. Associative behavior of hydrophobically modified hydroxyethyl celluloses (HMHECs) in waterborne coatings. *Prog Org Coat* **1993,** *22*, 245.

(19).Sun, W. B.; Sun, D. J.; Wei, Y. Q. Oil-in-water emulsions stabilized by hydrophobically modified hydroxyethyl cellulose: Adsorption and thickening effect. *J Colloid Interface Sci* **2007,** *311*, 228-236

(20) Krumora, M.; Lopez, D.; Benarente, R.; Mijangos, C.; Perena, J. M. Effect of crosslinking on the mechanical and thermal properties of poly(vinyl alcohol). *Polymer* **2000***, 41*, 9265–72.

(21) Nho, Y. C.; Moon, S. W.; Lee, K. H.; Park, C. W, Suh, T. S.; Jung, Y. J. Evaluations of poly(vinyl alcohol) hydrogels cross-linked under gamma-ray irradiation. *J Ind Eng Chem* **2005,** *11,* 159–64.

(22) Juang, J. H.; Bonner, W. S.; Ogawa, Y. J, Vacanti, P.; Weir, G. C. Outcome of subcutaneous is let transplantation improved by polymer device. *Transplantation* **1996,** *61*, 1557–61.

(23) Hyon, S. H.; Cha, W. I, Ikada, Y.; Kita, M.; Ogura, Y.; Honda, Y. Poly (vinyl alcohol) hydrogels as soft contact lens material. *J Biomater Sci Polym Ed* **1994,** *5*, 397–406. Kobayashi, M.; Oka, M. Composite device for attachment of polyvinyl alcohol-hydrogel to underlying bone. *Artif Organs* **2004,** *28*, 734–738.

(24) Zulkifli, F. H., Hussain, F. S. J., Rasad, M. S. B. A., & Yusoff, M. M. Improved cellular response of chemically crosslinked collagen incorporated hydroxyethyl cellulose/poly (vinyl) alcohol nanofibers scaffold. *J Biomat Appl*, 2014, 0885328214549818.

Zulkifli, F. H., Hussain, F. S. J., Rasad, M. S. B. A., & Yusoff, M. M. (2014). In vitro degradation study of novel HEC/PVA/collagen nanofibrous scaffold for skin tissue engineering applications. *Poly Degrade Stab*, **2014**, *110*, 473-481.

Chahal S; Hussain, F.S.J.; Yussof, M. Characterization of modified cellulose (MC)/poly (vinyl alcohol) electrospun nanofibers for bone tissue engineering. *Procedia Engineering*, 2013, ***53***, 683-688.

(25) Chahal, S.; Hussain, F.S.J.; Yussof, M. Biomimetic growth of bone-like apatite via simulated body fluid on hydroxyethyl cellulose/polyvinyl alcohol electrospun nanofibers. *Bio-Med Mater Eng* **2014,** 24, 799–806.

(26) Mavis, B.; Demirtaş, T. T.; Mşderelioğlu, M.; Gündüz, G.; Çolak, Ü. Synthesis, characterization and osteoblastic activity of polycaprolactone nanofibers coated with biomimetic calcium phosphate. *Acta Biomaterialia* **2009**, *5(8),* 3098-311119

(27) Beşkardeş, I. G.; Gümüşderelïoğlü, M. Biomimetic apatite-coated PCL scaffolds: effect of surface nanotopography on cellular functions. *J. Bioa. and Compat. Pol.* **2009**, *24*, 507-524.

(28) She, F. H.; Tung, K. L.; Kong, L. X. Calculation of effective pore diameters in porous filtration membranes with image analysis. *Robo. Comp.-Int. Manu.* **2008**, *24*, 427-434.

(29) Zhao, F.; Grayson, W. L.; Ma, T.; Bunnell, B.; Lu, W. W. Effects of hydroxyapatite in 3-D chitosan–gelatin polymer network on human mesenchymal stem cell construct development. *Biomaterials* **2006**, *27,* 1859–1867.

(30) Taboas, J. M.; Maddox, R. D.; Krebsbach, P. H.; Hollister, S. J. Indirect solid free form fabrication of local and global porous, biomimetic and composite 3D polymer-ceramic scaffolds. *Biomaterials* **2003,** *24,* 181–194.

(31) Schek, R. M.; Taboas, J. M.; Segvich, S. J.; Hollister, S. J.; Krebsbach, P. H. Engineered osteochondral grafts using biphasic composite solid free-form fabricated scaffolds. *Tiss. Eng.* **2004,** *10*, 1376–1385.

(32) Camargo, N. H. A.; Bellini, O. J.; Gemelli, E.; Tomiyama, M. Synthesis and characterization of nanostructures calcium phosphates powders and calcium phosphates/α-al2o3“ nanocomposites. *Revista Matériav*. **2007,** *12(4)*, 574 – 582.

(33) Tadashi, K.; Hiroaki, T. How useful is SBF in predicting in vivo bone bioactivity? *Biomaterials* **2006,** *27,* 2907–2915.

(34) Zheng, C. Y.; Li, S. J.; Tao, X. J.; Hao, Y. L.; Yang, R.; Zhang, L. Calcium phosphate coating of Ti–Nb–Zr–Sn titanium alloy. *Mat. Sci. Eng. C* **2007**, *27*, 824–831.

(35) Lee, J. S.; Choi, K. H.; Ghim, H. D.; Kim, S. S.; Chun, D. H.; Kim, H. Y.; Lyoo, W. S. Role of molecular weight of atactic poly(vinyl alcohol) (PVA) in the structure and properties of PVA nanofabric prepared by electrospinning. *J. Appl. Pol. Sci.* **2004,** *93(4),* 1638-1646.

(36) Shor, L.; Güçeria, S.; Wen, X.; Gandhi, M.; Sun, W. Fabrication of three-dimensional polycaprolactone/hydroxyapatite tissue scaffolds and osteoblast-scaffold interactions in vitro. *Biomaterials* **2007,** *28,* 5291–5297.

(37) Prabhakaran, M. P.; Venugopal, J.; Ramakrishna, S. Electrospun nanostructured scaffolds for bone tissue engineering. *Acta Biomaterialia* **2009,** *5*, 2884–2893

(38) Gupta, D.; Venugopal, J.; Mitra, S.; Giri Dev, V. R.; Ramakrishna, S. Nanostructured biocomposite substrates by electrospinning and electrospraying for the mineralization of osteoblasts. *Biomaterials* **2009**, *30*, 2085–2094

(39) Thomas, V.; Dean, D. R.; Jose, M. V.; Mathew, B.; Chowdhury, S.; Vohra, Y. K. Nanostructured biocomposite scaffolds based on collagen co-electrospun with nanohydroxyapatite. *Biomacromolecules* **2007,** *8*, 631-637.

(40) Ji, B.; Gao, H. Mechanical properties of nanostructure of biological materials. *J. Mech. Phy. Soli.* **2004**, *52*, 1963-1990.

(41) Rho, J. Y.; Kuhn-Spearing, L.; Zioupos, P. Mechanical properties and the hierarchical structure of bone. *Med. Eng. & Phy.* **1998**, *20*, 92-102.

(42) Linde, L.; Hvid, I. The effect of constraint on the mechanical behaviour of trabecular bone specimens. *J. Biomech.* **1989**, *22(5)*, 485-490.

(43) Rohlmann A.; Zilch, H.; Bergmann, G.; Kolbel, R. Material properties of femoral cancellous bone in axial loading. Part I: Time independent properties. *Arch. Orthop. Trauma Surg.* **1980,** *97(2), 95-102.*

(44) Shah D;, Maiti P; Jiang DD; Batt CA; Giannelis EP. Effect of nanoparticle mobility on toughness of polymer nanocomposites. *Adv Mater* **2005**; 17:525-8.

(45) Yang F; Both SK; Yang X; Walboomers XF; Jansen JA. Development of an electrospun nano-apatite/PCL composite membrane for GTR/GBR application. *Acta Biomaterialia* **2009**, 5; 3295–3304.

(46).Athanasiou, K.A; Zhu, C.F; Lanctot, D.R et al. 2000; Fundamentals of biomechanics in tissue engineering of bone. *Tissue Eng* 2000, **6**: 361–381.

(47) Fantner, G.E; Birkedal, H; Kindt, J.H et al. Influence of the degradation of the organic matrix on the microscopic fracture behavior of trabecular bone. *Bone* 2004, 35: 1013–1022.

(48) Ngiam, M., Liao, S., Patil, AJ., Cheng, Z., Chan, CK., Ramakrishna, S. The fabrication of nano-hydroxyapatite on PLGA and PLGA/collagen nanofibrous composite scaffolds and their effects on the osteoblastic behaviour for bone tissue engineering. *Bone*, **2009**, **45**: 4-16.

(49) Zhang, W.; Huang, KL.; Liao, SS.; Cui, FZ. Nucleation sites of calcium phosphate crystals during collagen mineralization. *J Am Ceram Soc* **2003**; 86:1052–4

(50) Weiner S; Wagner, HD. The material bone: structure–mechanical function relations. *Ann Revie Mater Sci*, 1998. **28**:271–98.

(51) Fratzl P; Weinkamer, R. Nature’s hierarchical materials. *Prog Mater Sci*, 2007, **52**; 1263–334.

(52) Rho, JY; Kuhn-Spearing L; Zioupos, P. Mechanical prperties and the hierarchical structure of bone. *Med Eng Phy*, 1998; **20**; 92–102.

Graphical abstract

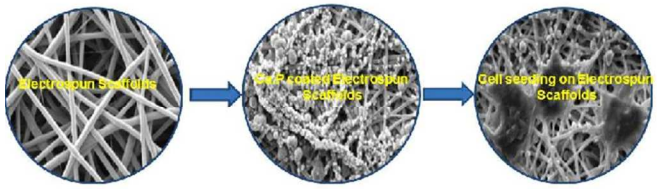

Calcium phosphate coated HEC/PVA nanofibrous scaffolds for bone tissue engineering applications.